Electronic Supplementary Information for

Pyrazolium ionic liquids with multiple active sites immobilized on mesoporous MCM-41 for chemical fixation of CO_2 under mild conditions

Jean Damascene Ndayambaje [a, b], Irfan Shabbir [a, b], Li Dong [a], Qian Su [a]*, Weiguo Cheng [c, a]*

[a] CAS Key Laboratory of Green Process and Engineering, State Key Laboratory of Multiphase Complex Systems, Beijing Key Laboratory of Ionic Liquids Clean Process, Institute of Process Engineering, Chinese Academy of Sciences, Beijing 100190 (China)

[b] University of Chinese Academy of Sciences, Beijing 100190 (China)

[c] Zhengzhou Institute of Emerging Industrial Technology, Zhengzhou, Henan 450000, China

*Corresponding authors.

Prof. Weiguo Cheng: wgcheng@ipe.ac.cn

Dr. Qian Su: qsu@ipe.ac.cn

1. Detailed experimental procedure

1.1. Materials

Reagents and chemicals such as cetyltrimethylammonium bromide (CTAB), tetraethylorthosilicate (TEOS), (3-Aminopropyl) triethoxysilane, benzene, 2,2'-azobisisbutyronitrile, 1-Methylpyrazole, acetonitrile, ethyl acetate, and ethanol; various epoxides including propylene oxide (PO), styrene oxide (SO), epichlorohydrin (ECH), allyl glycidyl ether (AGE), glycidol, 1,2-butylene oxide (BO), and the internal epoxide of cyclohexene oxide (CHO); different alkyl chain lengths such as 1,6-dibromohexane, 1,5-dibromopentaane, 1,4-dibromobutane, and 1,3-dibromopropane were of analytical grade and were obtained from Shanghai Aladdin Chemical Company with a purity of over 98%. All purity of chemicals was the Analytical reagent. No additional purification was conducted. CO_2 and N_2 gases with a purity of 99.95% were supplied by Beijing Analytical Instrument Factory.

1.2. Synthesis of dicationic pyrazolium ILs

The preparation of 2,2'-(hexane-1,6-diyl)-bis(1-methylpyrazolium) dibromide (C_6Pz) has been slightly modified with reference to the literature [1] as follows: Firstly, 4.105 g of 1-methylpyrazole (50 mmol) was added to 18 mL of CH_3CN in a 100 mL three-necked flask and stirred at room temperature for 1 hour. Next, 12.2 g of 1,6-dibromohexane (50 mmol) was added, and the mixture was stirred under nitrogen protection at 80 °C for 30 hours. At the end of the reaction, the remaining solvent was evaporated with a rotary evaporator. The resulting residue was then washed with a 1:1 solution of ethanol and ethyl acetate (10 mL x 4) and purified by centrifugation to remove impurities. Ultimately, the pure white solid (C_6Pz) was acquired and dried in a vacuum oven at 60 °C for 20 h. Other

DPzILs were prepared by the same method. A comprehensive list of ^{1}H NMR data for DPzILs is provided below, demonstrating the preservation of all characteristic peaks. Additionally, the structures and ^{1}H NMR spectra of DPzILs are shown in Figures S1-S5. C_6Pz: ^{1}H NMR (600 MHz, Deuterium Oxide) δ 8.22 – 8.10 (m, 2H), 6.77 – 6.69 (m, 2H), 4.43 (td, J = 7.4, 1.6 Hz, 2H), 4.11 (d, J = 2.8 Hz, 6H), 3.47 (t, J = 6.7 Hz, 4H), 1.95 – 1.79 (m, 4H), 1.53 – 1.33 (m, 4H). 2,2'-(pentane-1,5-diyl)-bis(1-methylpyrazolium) dibromide (C_5Pz): ^{1}H NMR (600 MHz, Deuterium Oxide) δ 8.23 – 8.06 (m, 2H), 6.71 (t, J = 3.0 Hz, 2H), 4.41 (t, J = 7.4 Hz, 2H), 4.09 (s, 6H), 3.22 (t, J = 6.8 Hz, 4H), 2.08 – 1.71 (m, 2H), 1.47 – 1.27 (m, 4H). 2,2'-(butane-1,4-diyl)-bis(1-methylpyrazolium) dibromide (C_4Pz): ^{1}H NMR (600 MHz, Deuterium Oxide) δ 8.18 (dd, J = 32.3, 3.0 Hz, 2H), 6.74 (q, J = 2.8 Hz, 2H), 4.56 – 4.43 (m, 2H), 4.11 (s, 6H), 3.51 (t, J = 6.4 Hz, 4H), 2.11 – 1.86 (m, 4H). 2,2'-(propane-1,3-diyl)-bis(1-methylpyrazolium) dibromide (C_3Pz): ^{1}H NMR (600 MHz, Deuterium Oxide) δ 8.26 – 8.10 (m, 2H), 6.74 (t, J = 3.0 Hz, 2H), 4.56 – 4.42 (m, 2H), 4.12 (s, 6H), 3.27 (t, J = 6.7 Hz, 2H), 2.09 – 1.83 (m, 4H).

1.3. Computational details

Density functional theory (DFT) calculations performed by the Gaussian 09 program package [2] were employed to investigate the interactions of PO and DPzILs catalysts. The reactants, intermediates, transition states, and products geometries were optimized using the B3LYP method and 6-31+G(d,p) basis set (B3LYP/6-31+G(d,p)), and subsequent frequency calculations at the same level confirmed the optimized structures as ground states without imaginary frequencies (NImag = 0). Vibrational frequency with only one imaginary frequency stands for the transition state.

2. Experimental results

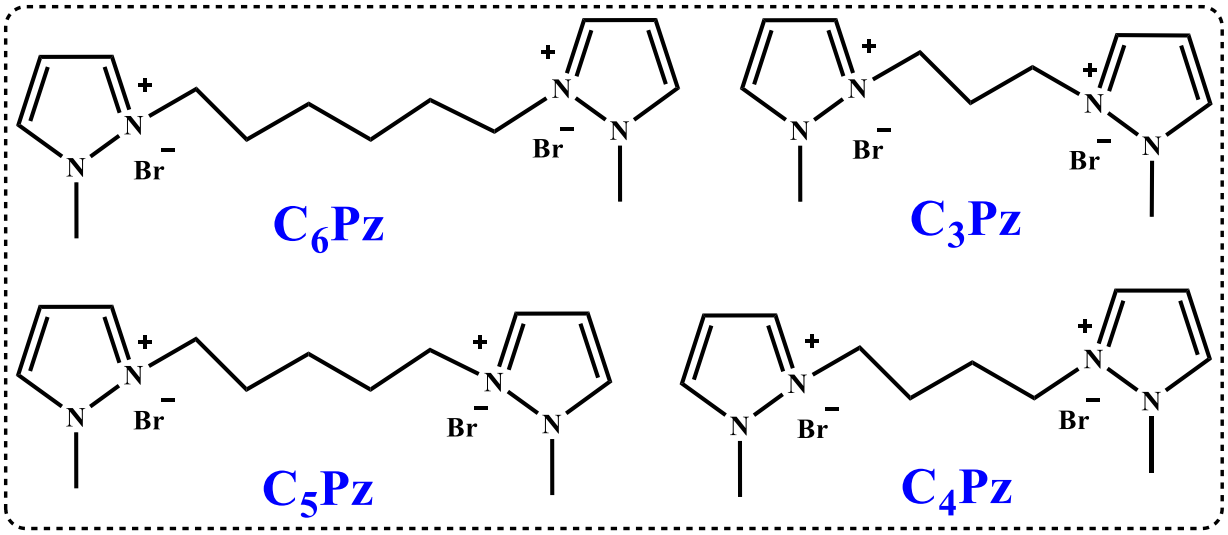

Figure S1. Structures of dicationic pyrazolium ionic liquids

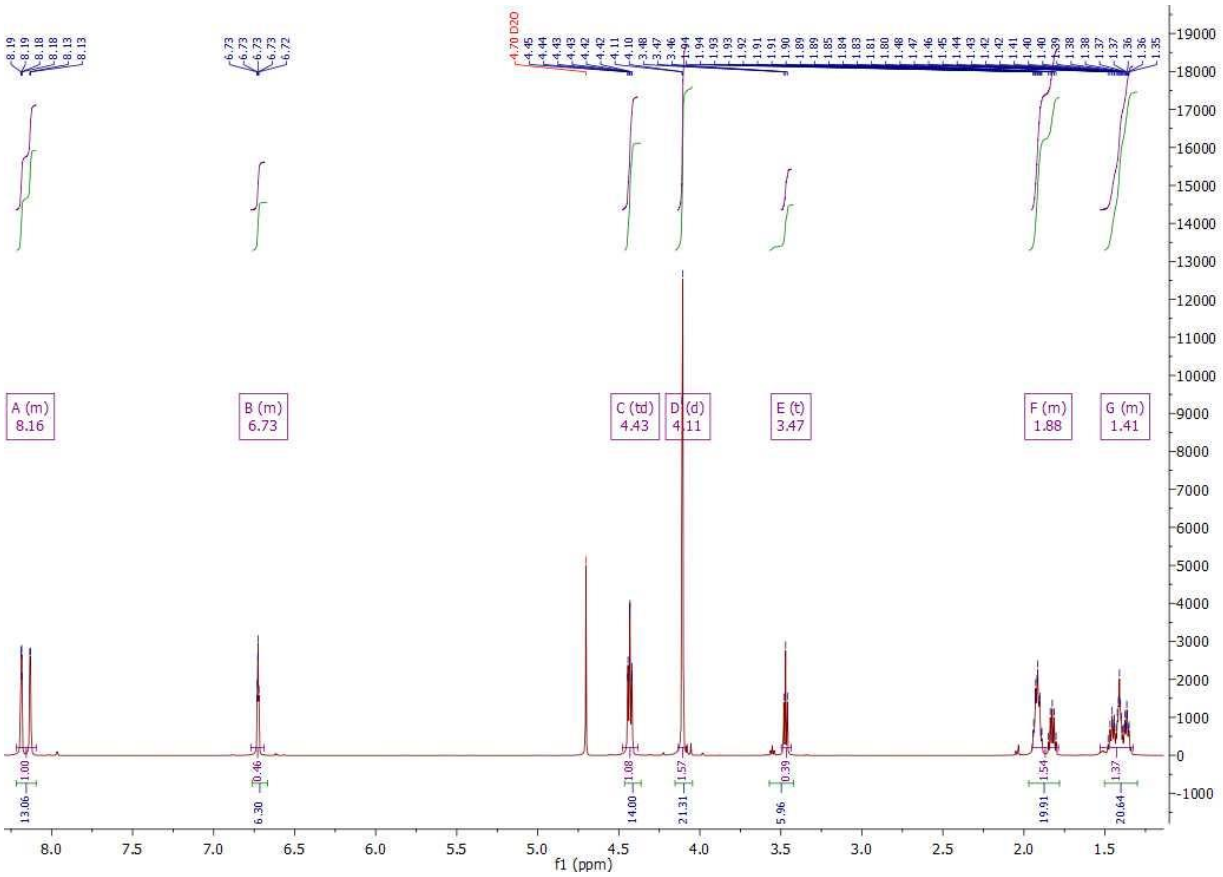

Figure S2. ^{1}H NMR spectrum of C_6Pz

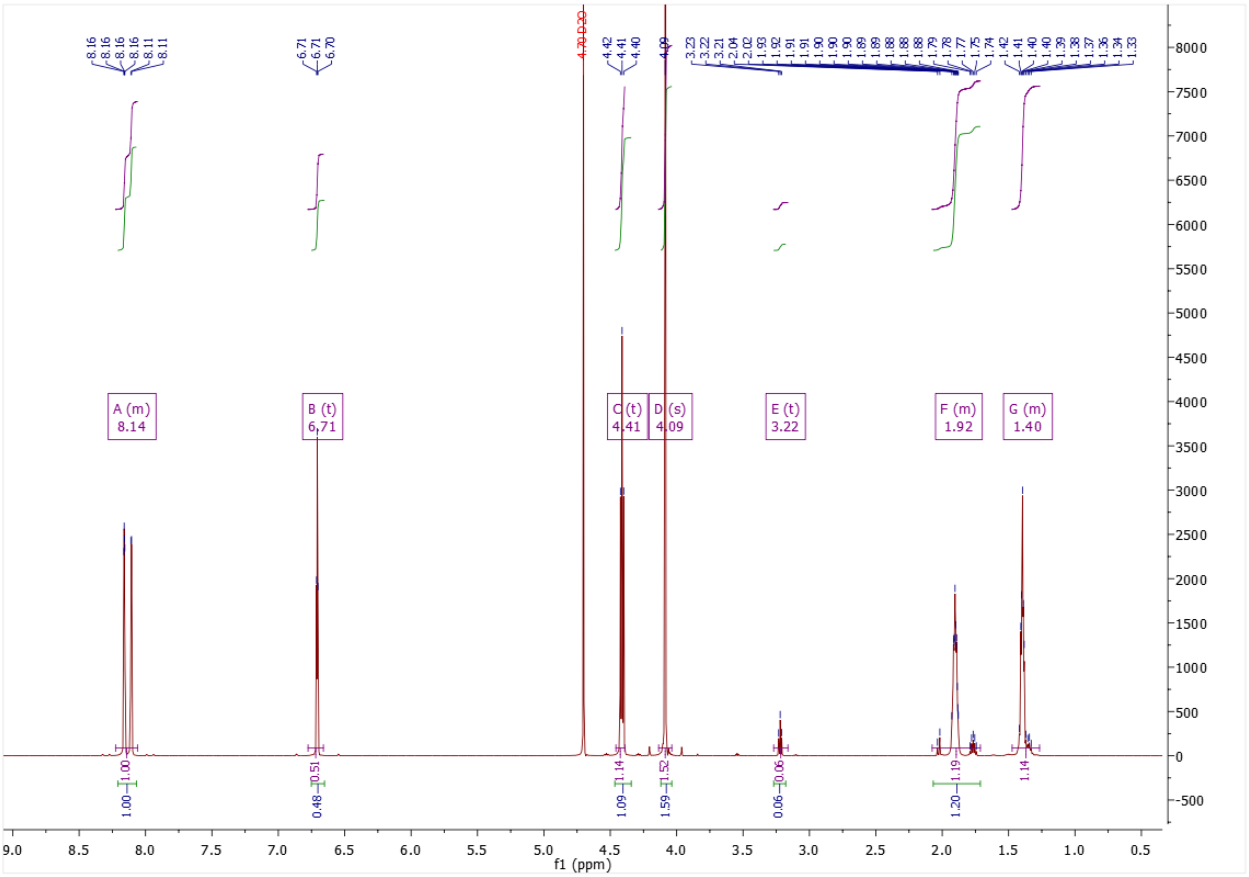

Figure S3. ^{13}C NMR spectrum of C_5Pz

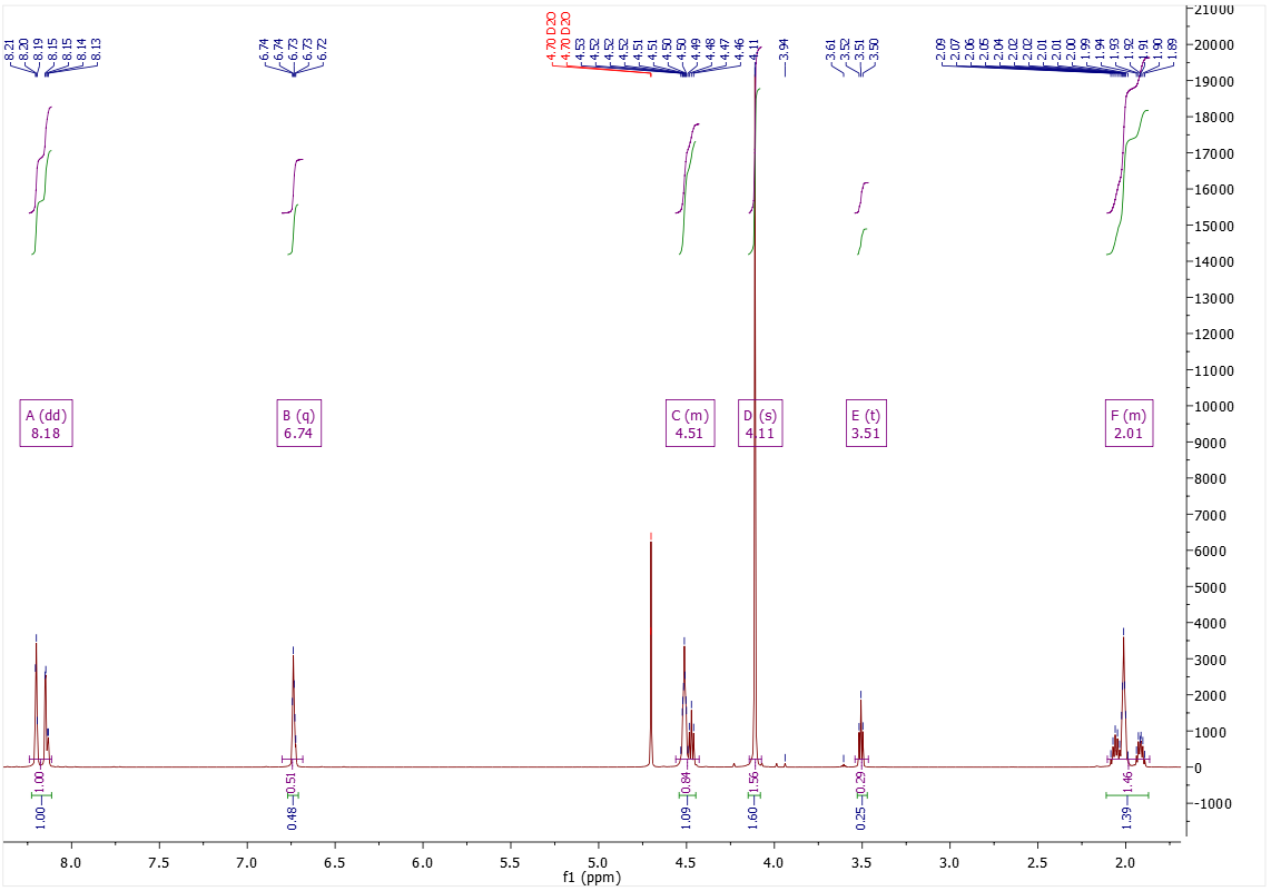

Figure S4. ^{1}H NMR spectrum of C_4Pz

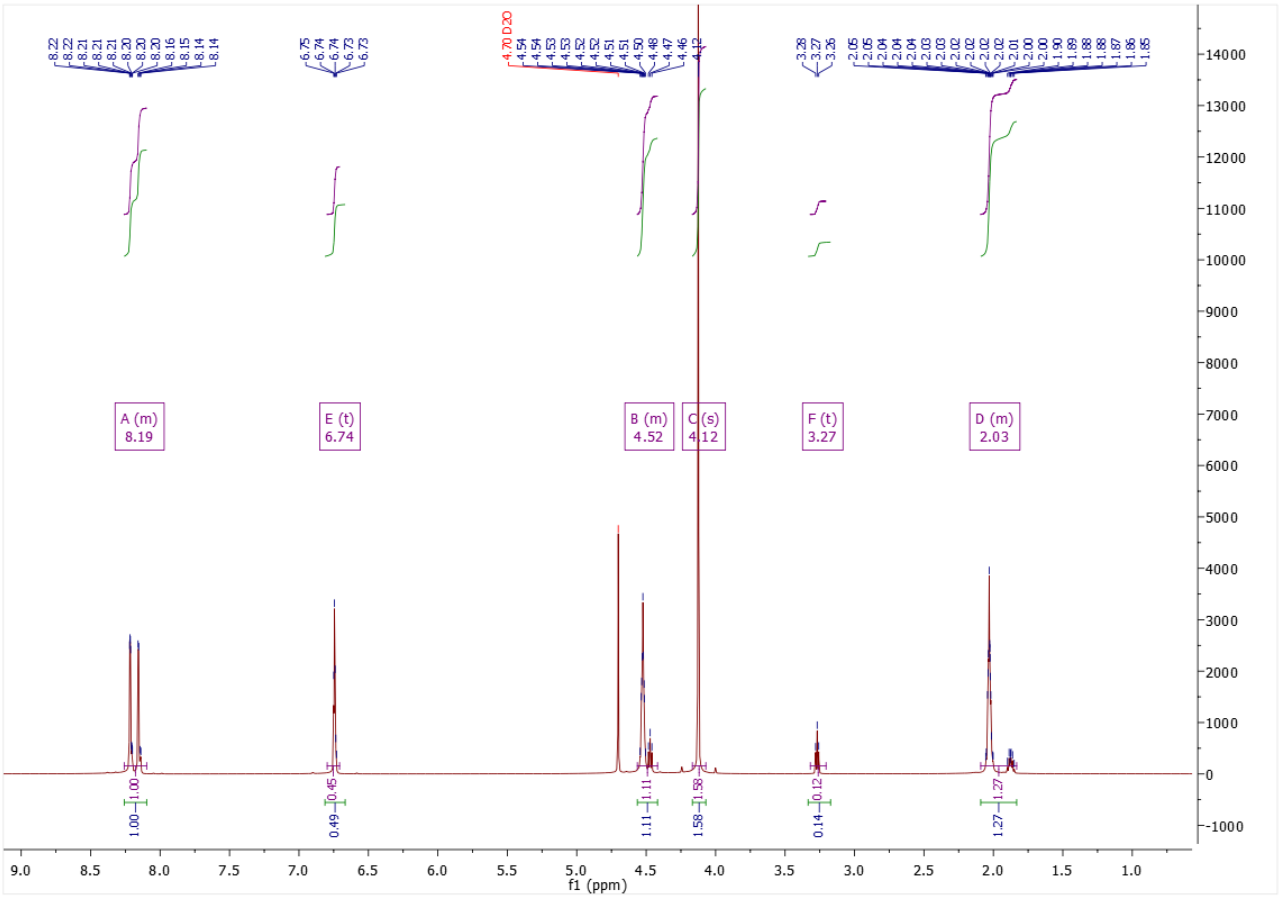

Figure S5. ^{1}H NMR spectrum of C_3Pz

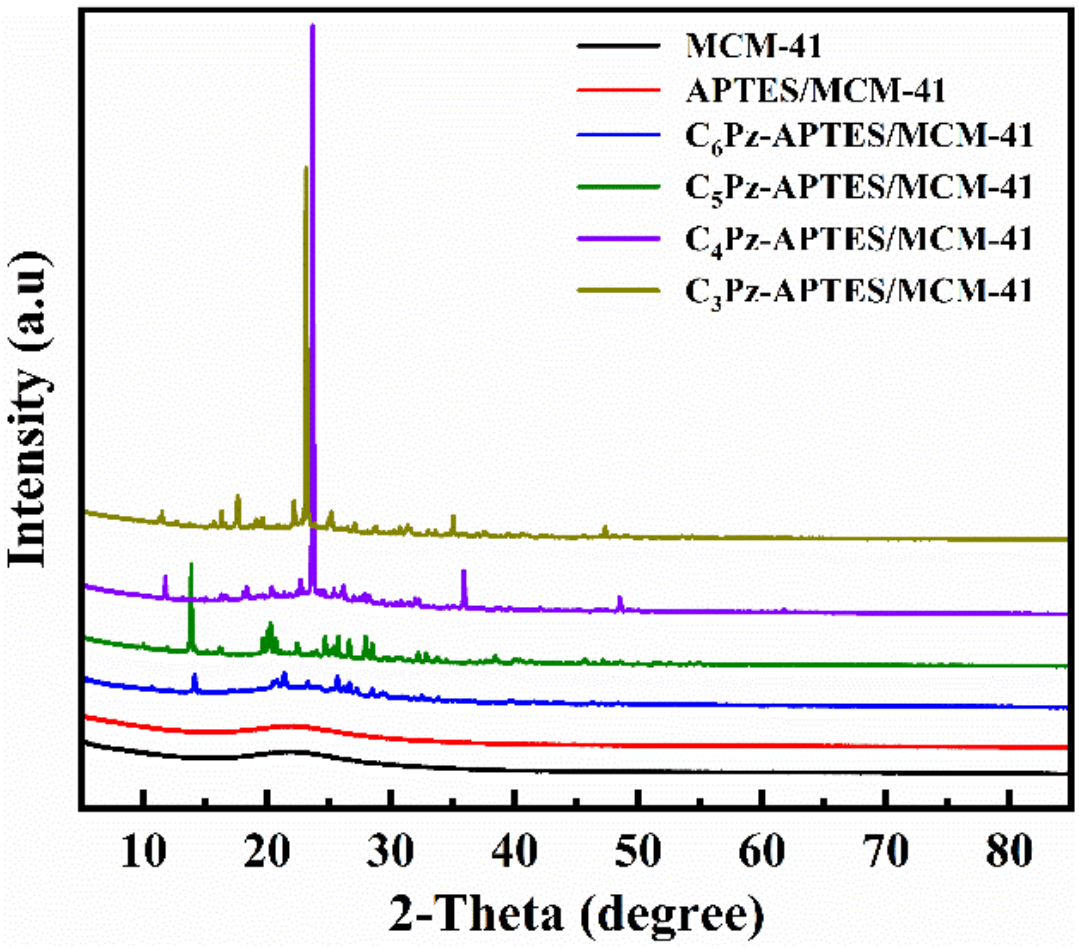

Figure S6. WAXRD patterns of MCM-41, APTES/MCM-41, and IDPzILs.

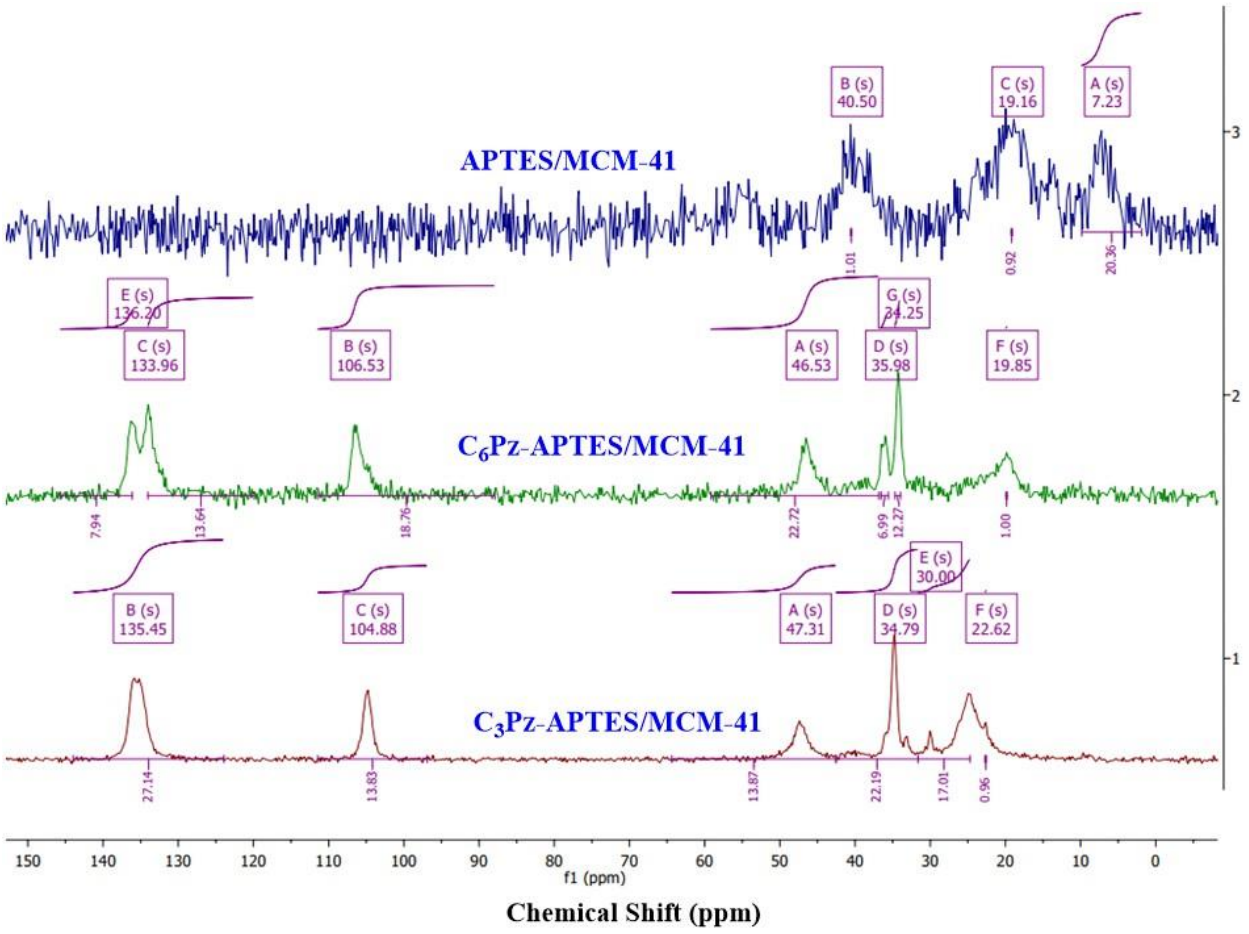

Figure S7. The ^{13}C MAS NMR spectra for APTES/MCM-41, C_3Pz-APTES/MCM-41, and C_6Pz-APTES/MCM-41

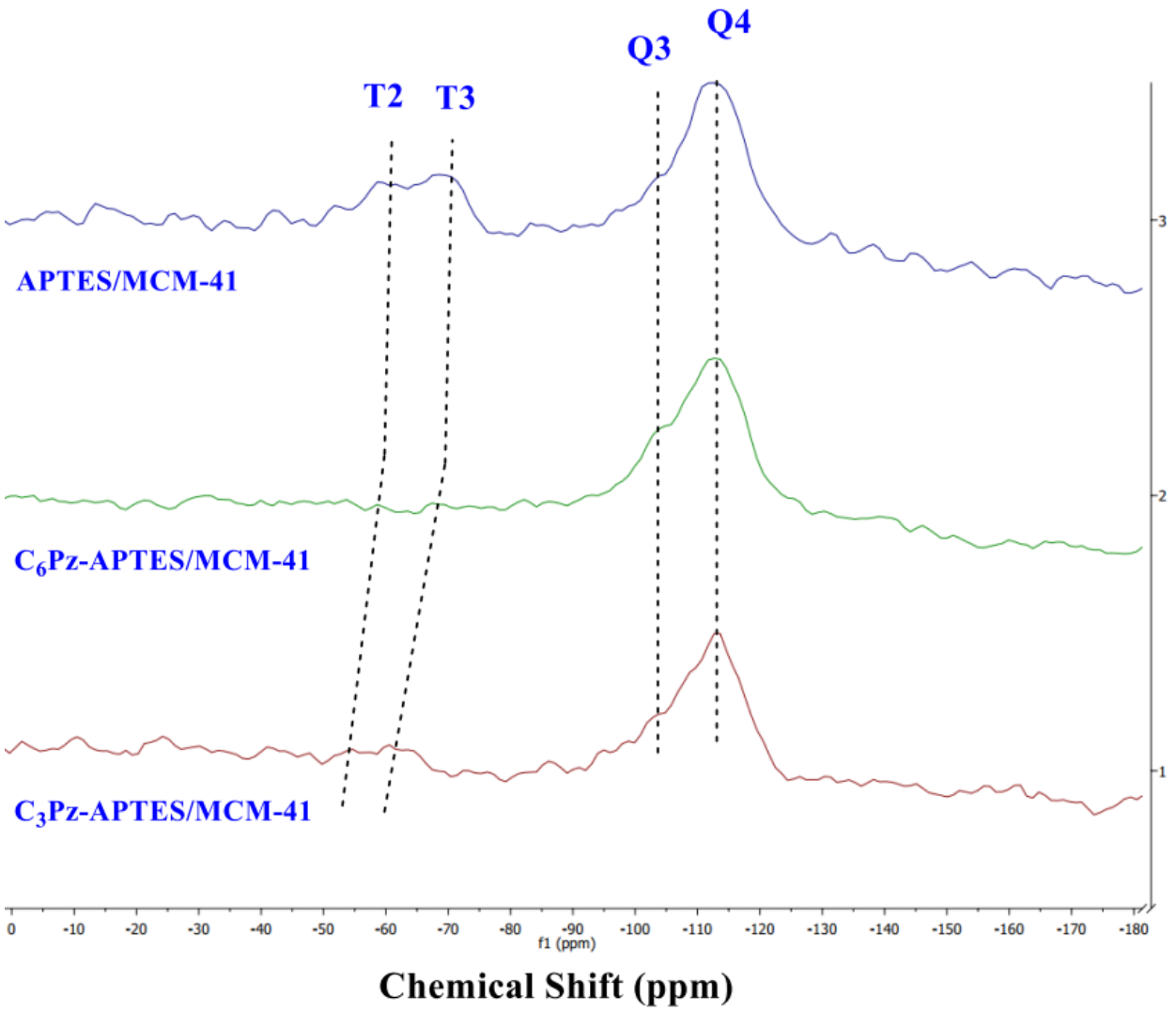

Figure S8. The ^{29}Si MAS NMR spectra for APTES/MCM-41, C_3Pz-APTES/MCM-41, and C_6Pz-APTES/MCM-41

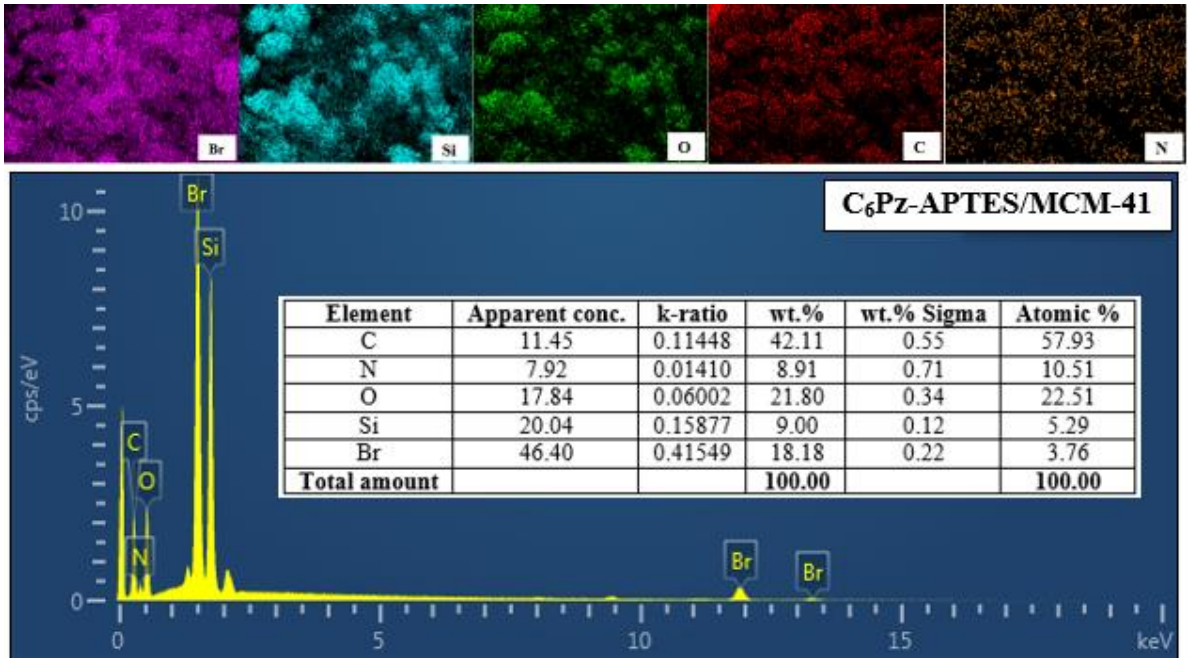

Element	Apparent conc.	k-ratio	wt.%	wt.% Sigma	Atomic %
C	11.45	0.11448	42.11	0.55	57.93
N	7.92	0.01410	8.91	0.71	10.51
O	17.84	0.06002	21.80	0.34	22.51
Si	20.04	0.15877	9.00	0.12	5.29
Br	46.40	0.41549	18.18	0.22	3.76
Total amount			**100.00**		**100.00**

Figure S9. EDS profile of C_6Pz-APTES/MCM-41

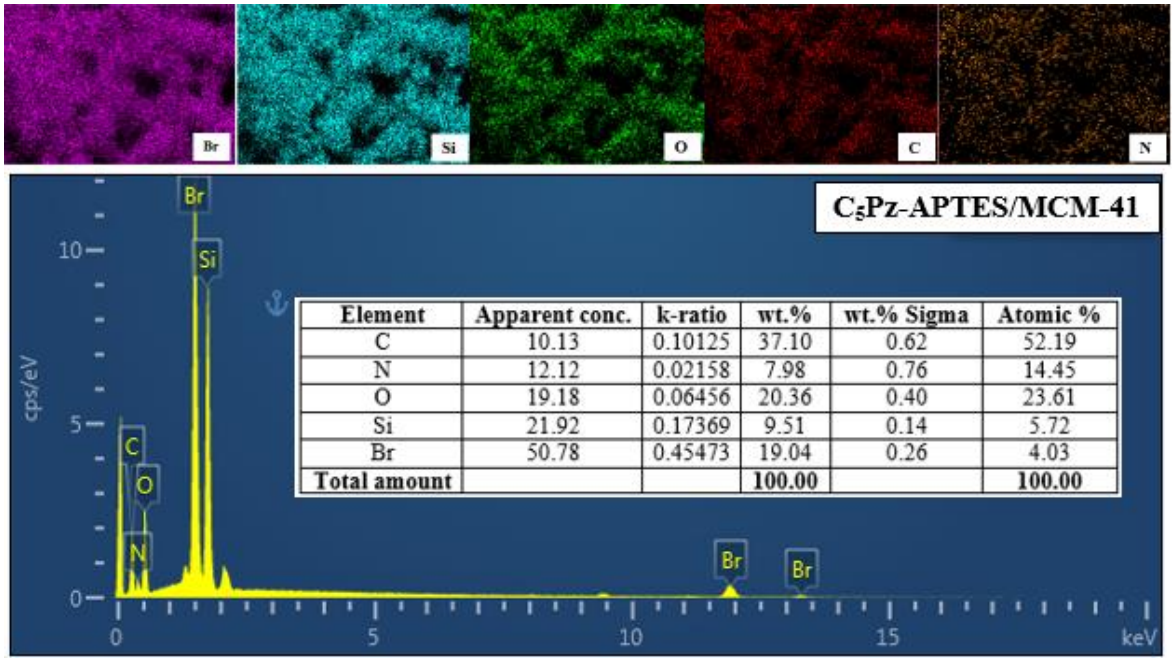

Element	Apparent conc.	k-ratio	wt.%	wt.% Sigma	Atomic %
C	10.13	0.10125	37.10	0.62	52.19
N	12.12	0.02158	7.98	0.76	14.45
O	19.18	0.06456	20.36	0.40	23.61
Si	21.92	0.17369	9.51	0.14	5.72
Br	50.78	0.45473	19.04	0.26	4.03
Total amount			**100.00**		**100.00**

Figure S10. EDS profile of C_5Pz-APTES/MCM-41

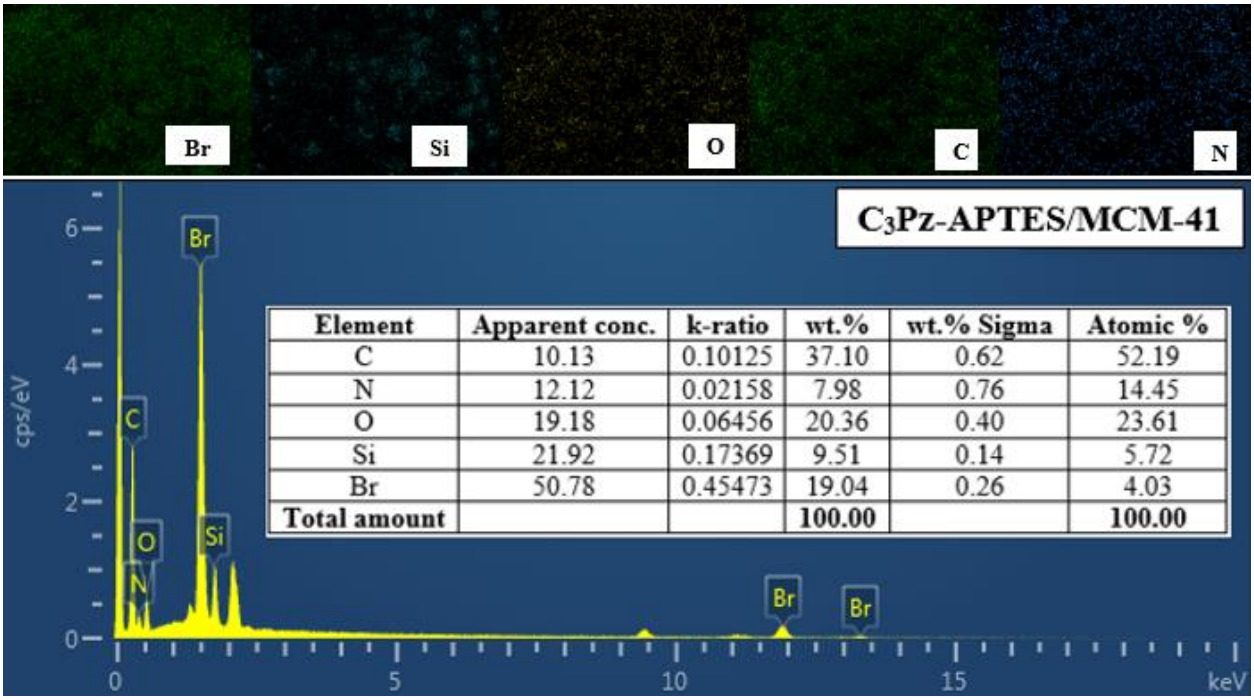

Element	Apparent conc.	k-ratio	wt.%	wt.% Sigma	Atomic %
C	10.13	0.10125	37.10	0.62	52.19
N	12.12	0.02158	7.98	0.76	14.45
O	19.18	0.06456	20.36	0.40	23.61
Si	21.92	0.17369	9.51	0.14	5.72
Br	50.78	0.45473	19.04	0.26	4.03
Total amount			**100.00**		**100.00**

Figure S11. EDS profile of C_3Pz-APTES/MCM-41

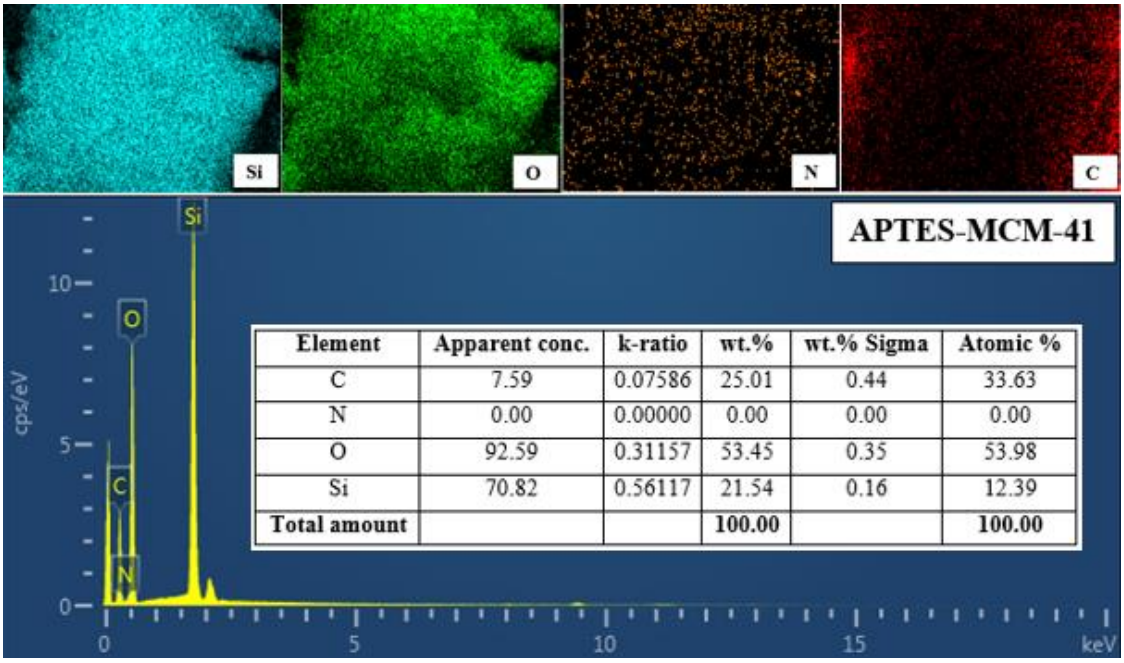

Element	Apparent conc.	k-ratio	wt.%	wt.% Sigma	Atomic %
C	7.59	0.07586	25.01	0.44	33.63
N	0.00	0.00000	0.00	0.00	0.00
O	92.59	0.31157	53.45	0.35	53.98
Si	70.82	0.56117	21.54	0.16	12.39
Total amount			**100.00**		**100.00**

Figure S12. EDS profile of APTES/MCM-41

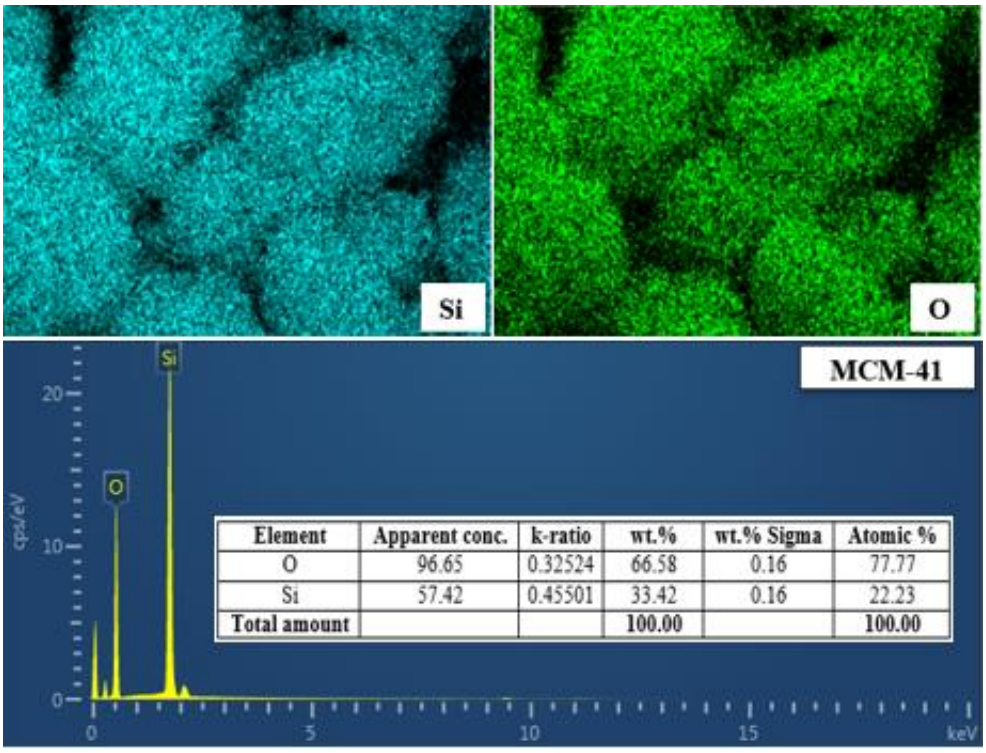

Figure S13. EDS profile of MCM-41 molecular sieve

3. Effect of reaction parameters

3.1. Effect of reaction temperature

The primary reaction parameters for coupling CO_2 with PO to cyclic carbonate were thoroughly investigated, including the reaction temperature, catalyst amount, CO_2 pressure, and reaction time, as illustrated in Figure S13. The catalytic activity of C_6Pz-APTES/MCM-41 was examined as a case study. It was found that the appropriate increase of reaction temperature, catalyst dosage, and reaction time is beneficial to improve the product PC yield, and the PC yields of IDPzILs are all higher than 95.0% under the reaction conditions of 90 °C, 0.2 g of catalyst, and 3 hours. Figure S13(A) displays the results of experiments designed to illustrate the impact of reaction temperature. The results indicate an increasing trend in PC yield and selectivity.

Increasing the reaction temperature from 80 °C to 90 °C resulted in a 40.8% increase in PC yield. The data indicate a gradual increase in product yield within the temperature range of 60–80 °C and 90–130 °C, with values rising from 16.8% to 53.0% and 93.8% to 97.0%, respectively. The product yield increases significantly from 53.0% to 93.8% within the 80–90 °C range. Then, with a further increase in temperature, the PC yield experienced a marginal increase from 93.8% to 97.0% within the temperature interval of 90–130 °C. Regarding selectivity, the C_6Pz-APTES/MCM-41 catalyst showed remarkable stability, maintaining a level above 99.3% throughout the process.

3.2. Effect of CO_2 pressure

As shown in Figure S13(B), the pressure of CO_2 significantly affects the catalytic activity. The increase in PC production was 63.8% when the CO_2 pressure was changed within the range of 0.1 to 0.5 MPa. The PC yield achieved at a carbon dioxide pressure of 1.0 MPa was determined to be 95.6%. Therefore, a pressure of 1.0 MPa is the optimal choice. However, a slight decrease was observed when the CO_2 pressure reached 1.0 MPa, resulting in PC production percentages of 82.0%, 78.3%, and 80.6% for CO_2 pressures of 1.5 MPa, 2.0 MPa, and 2.5 MPa, respectively. Increasing the CO_2 pressure would initially elevate the reactant concentration and facilitate the catalytic process. Introducing more CO_2 into the system would decrease the concentration of IDPzILs, causing a partial suppression of the reaction and ultimately leading to a drop in the yield of the desired product. Furthermore, the substrate (PO in our work) can be diluted due to the high CO_2 concentration, leading to decreased reaction rates [3]. Throughout this experimental process, it is important to highlight that the selectivity remained consistent and robust, exceeding 99%. This underscores the precision and effectiveness of the catalytic process under varying CO_2 pressures.

3.3. Effect of catalyst amount

Another aspect examined was the influence of catalyst loading on the synthesis of PC and its selectivity. As depicted in Figure S13(C), there is a notable increase in the percentage of PC produced as the amount of catalyst employed increases, with values rising from 69.1% to 88.7% as the catalyst amount escalates from 0.05 g to 0.2 g. When the quantity of C_6Pz-APTES/MCM-41 was increased from 0.2 g to 0.3 g, the resulting product exhibited a PC yield of 95.5% and a selectivity of 99.9%. Despite the increase in the catalyst amount from 0.3 g to 0.5 g, the experimental findings indicate that the product yield remained reasonably constant, ranging from 95.4% to 97.1%. Comparably, the results from all trials showed a selectivity rate of over 99%. The optimal amount of catalyst for the reaction was determined to be 0.3 g (14.7 wt.%).

3.4. Effect of reaction time

Figure S13(D) shows how PC yield and selectivity change with reaction time. A significant increase in PC yield was observed within the first three hours, from 49.5% to 75.5%. Extending the reaction time may contribute to some degree of CO_2 sequestration. After 4 h of reaction, the yield reaches a high percentage of 97.2%. This indicates that most of the reactants have been converted to propylene carbonate and the reaction is nearly complete. The yield increases slightly to 97.7% after 6 h. This small increase indicates that the reaction has reached an optimal time. The system consistently showed selectivity above 99.8% regardless of reaction time. In summary, the optimal conditions for this reaction are a temperature of 90 °C, a CO_2 pressure of 1.0 MPa, a catalyst weight of 0.3 g, and a reaction time of 4 h. The investigation was concluded by comparing the activity of the C_6Pz-APTES/MCM-41 catalyst with that of previously known grafted catalysts to evaluate the advantages of the catalytic efficiency of this catalyst (Table S2). The data presented

in this work show that under mild reaction conditions, C_6Pz-APTES/MCM-41 exhibits the properties of a sustainable and efficient catalyst for the environmentally benign conversion of CO_2 and epoxides to cyclic carbonates [4-8].

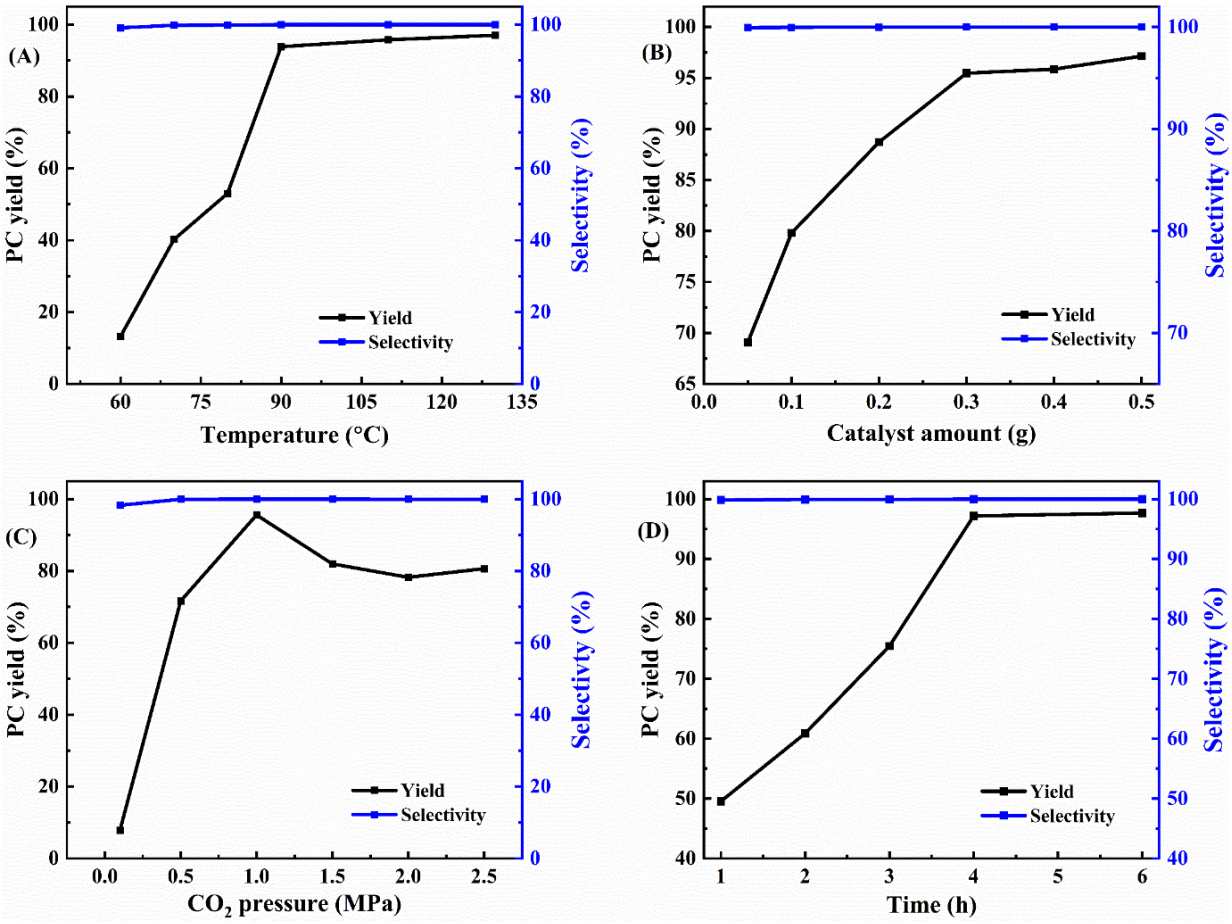

Figure 14. Effects of different parameters on the PC yield and selectivity catalyzed by C_6Pz-APTES/MCM-41: (A) Effect of reaction temperature (reaction conditions: PO 30 mmol, catalyst 0.2 g, initial CO_2 pressure 1.0 MPa, time 3 h); (B) Effect of catalyst amount on PC yield and selectivity (reaction conditions: PO 30 mmol, temperature 90 °C, initial CO_2 pressure 1.0 MPa, time 3 h); (C) Effect of CO_2 pressure on PC yield and selectivity (reaction conditions: PO 30 mmol, catalyst 0.3 g, temperature 90 °C, time 3 h); (D) Effect of reaction time on PC yield and selectivity (reaction conditions: PO 30 mmol, catalyst 0.3 g, temperature 90 °C, initial CO_2 pressure 1.0 MPa).

3.4. Effect of reaction time

Figure S13(D) shows how PC yield and selectivity change with reaction time. A significant increase in PC yield was observed within the first three hours, from 49.5% to 75.5%. Extending the reaction time may contribute to some degree of CO_2 sequestration. After 4 h of reaction, the yield reaches a high percentage of 97.2%. This indicates that most of the reactants have been converted to propylene carbonate and the reaction is nearly complete. The yield increases slightly to 97.7% after 6 h. This small increase indicates that the reaction has reached an optimal time. The system consistently showed selectivity above 99.8% regardless of reaction time. In summary, the optimal conditions for this reaction are a temperature of 90 °C, a CO_2 pressure of 1.0 MPa, a catalyst weight of 0.3 g, and a reaction time of 4 h. The investigation was concluded by comparing the activity of the C_6Pz-APTES/MCM-41 catalyst with that of previously known grafted catalysts to evaluate the advantages of the catalytic efficiency of this catalyst (Table S2). The data presented in this work show that under mild reaction conditions, C_6Pz-APTES/MCM-41 exhibits the properties of a sustainable and efficient catalyst for the environmentally benign conversion of CO_2 and epoxides to cyclic carbonates [4-8].

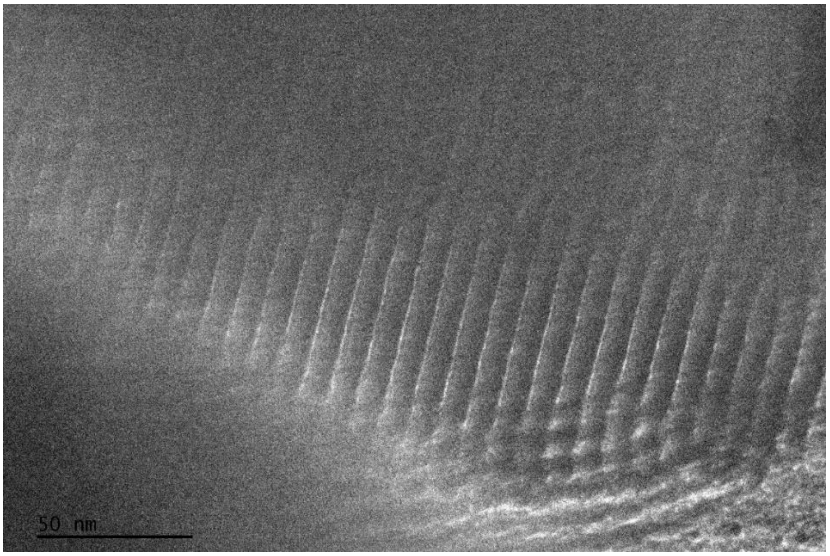

Figure S15. The TEM image of reused C_6Pz-APTES/MCM-41

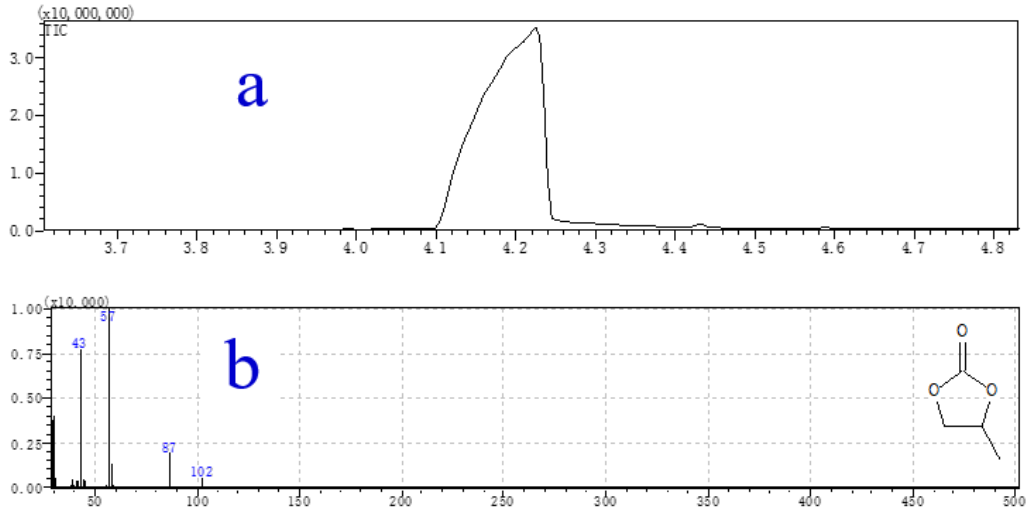

Figure S16. The chromatogram (a) and mass spectrum (b) of the product, propylene carbonate.

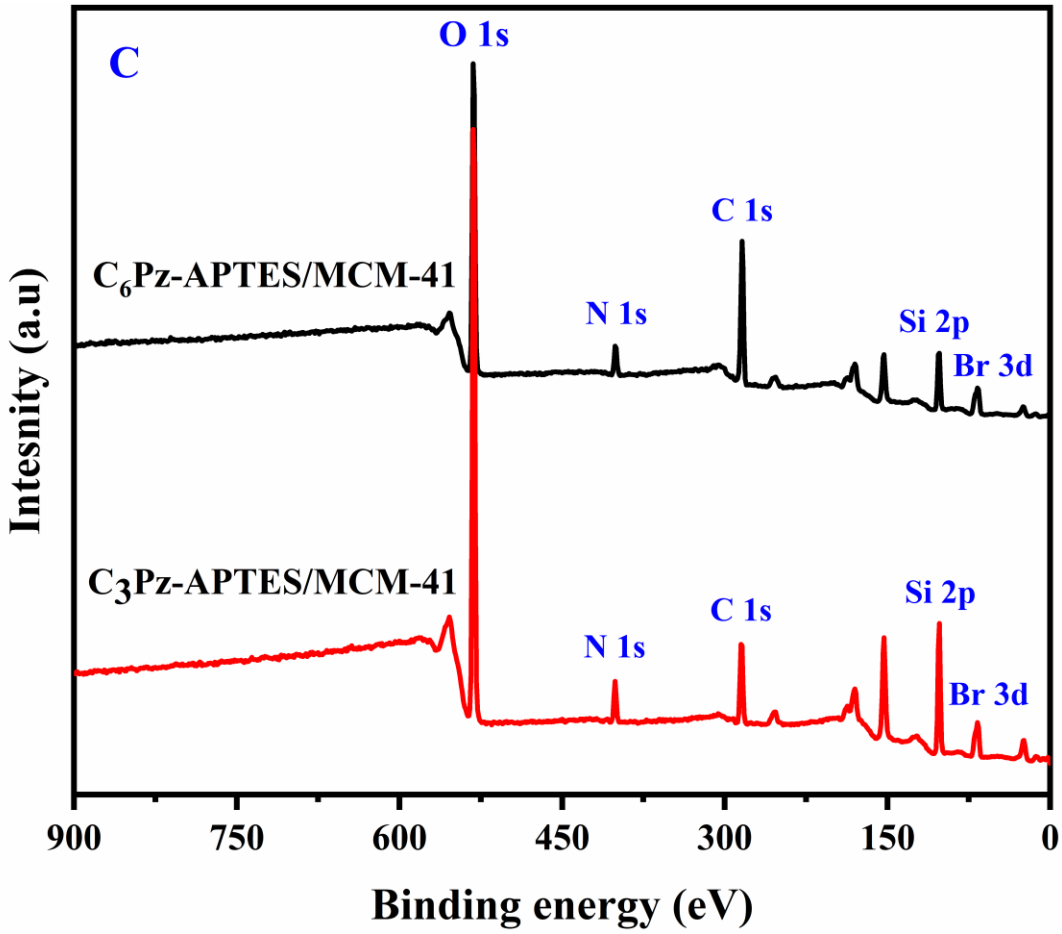

Figure S17. XPS survey spectra for C_6Pz-APTES/MCM-41 and C_3Pz-APTES/MCM-41

4. Optimized structures and bond distances between PO and DPzILs

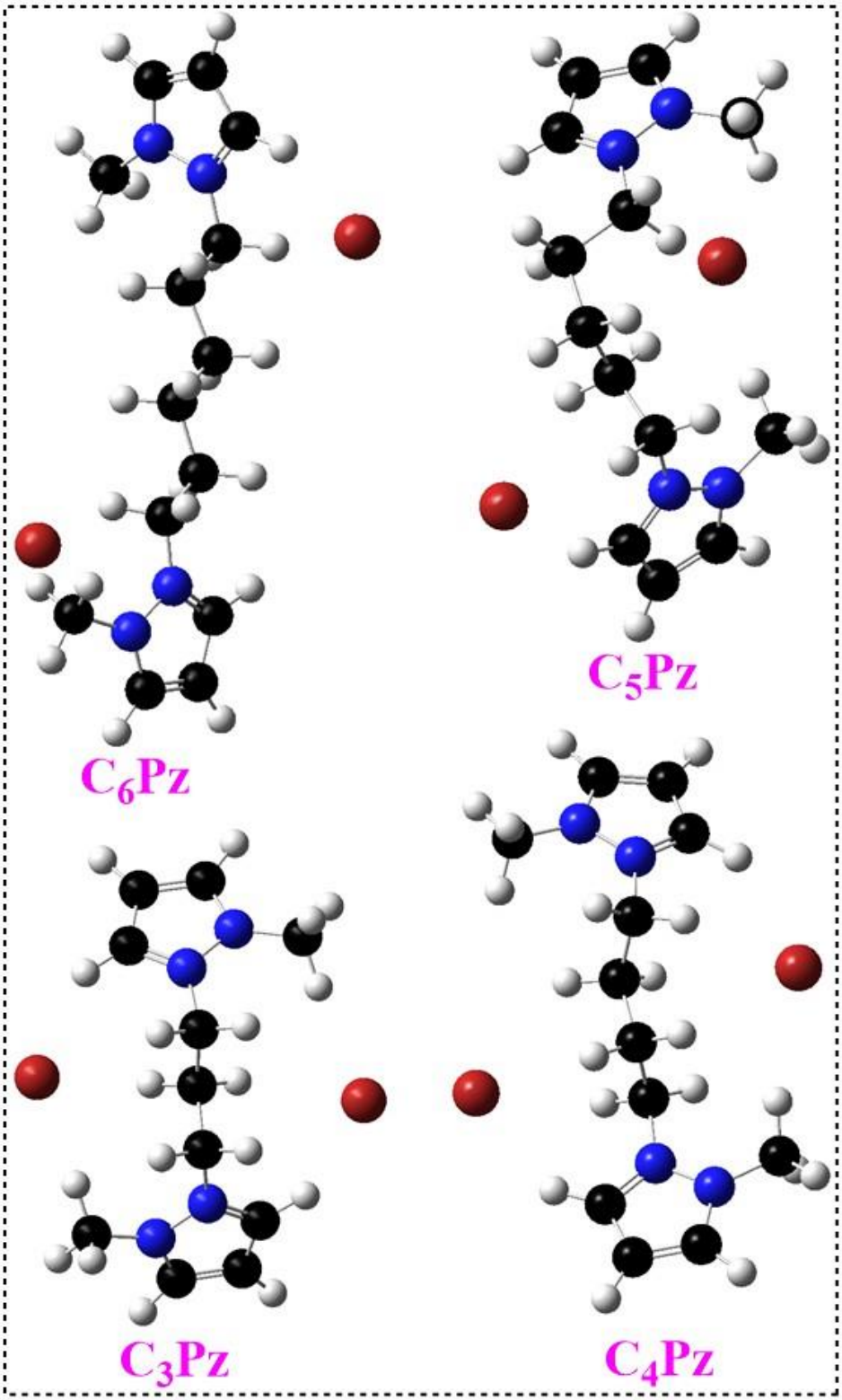

Figure S18. Optimized structures of the bulk ILs computed at the B3LYP/6-31+G(d,p) set level.

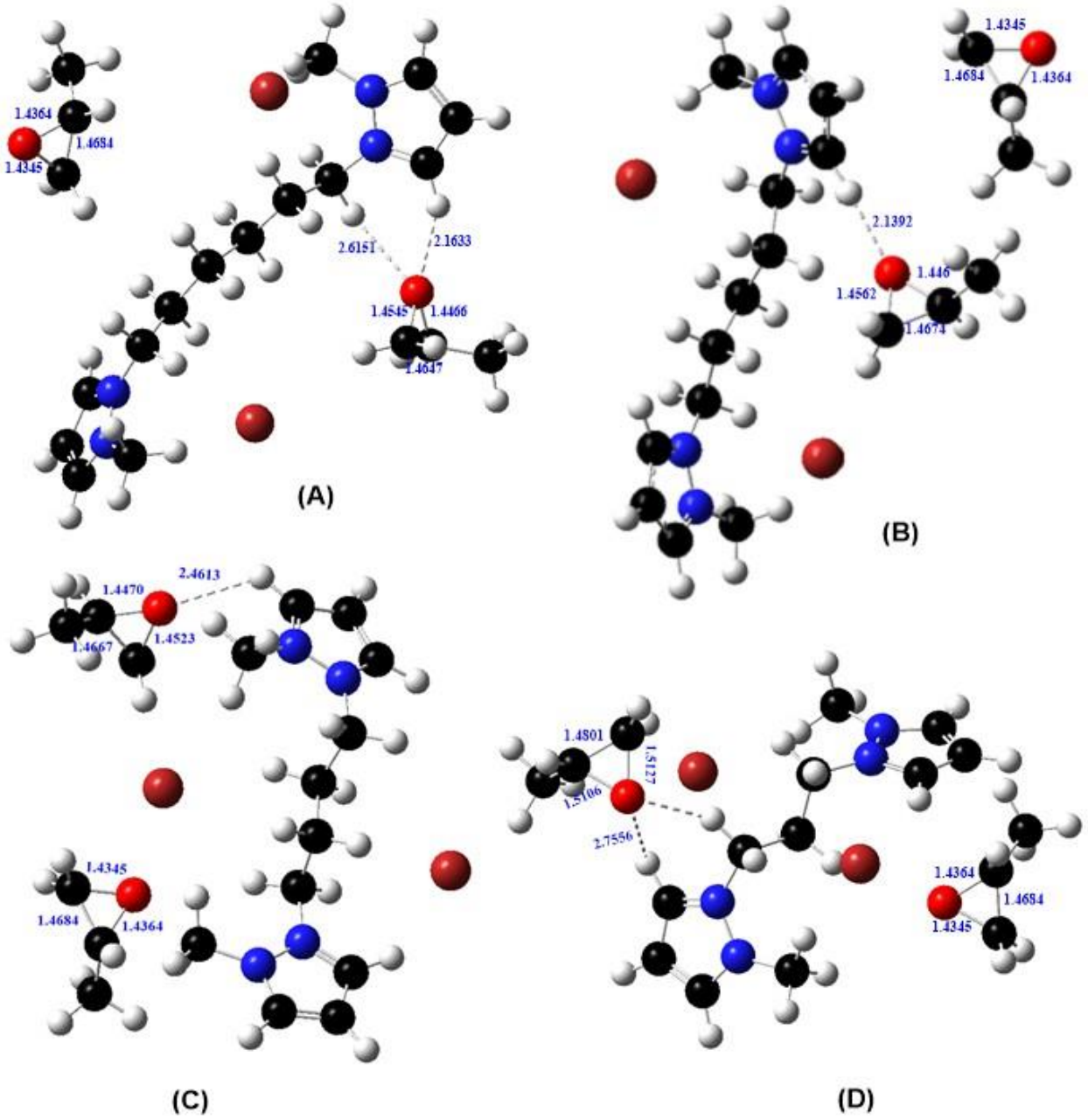

Figure S19. The bond distances between PO and DPzILs, in angstrom (Å). The optimized geometries for PO and DPzILs were computed at the B3LYP/6-31+G (d,p) set level: C_6Pz-PO (A), C_5Pz-PO (B), C_4Pz-PO (C), and C_6Pz-PO (D).

Table S1. Catalytic activity for coupling reaction of PO and CO_2.[a]

Entry	Catalyst	*T* (°C)	CO_2 (MPa)	Time (h)	Yield (%)[b]	Sel. (%)[b]	TOF (h^{-1})[c]
1	C_3Pz-APTES/MCM-41	80	1.0	4	85.1	99.9	45.6
2	C_6Pz-APTES/MCM-41	80	1.0	4	93.2	99.9	49.9
3	C_3Pz-APTES/MCM-41	130	1.0	2	86.1	99.6	109.8
4	C_4Pz-APTES/MCM-41	130	1.0	2	91.3	99.9	120.4
5	C_5Pz-APTES/MCM-41	130	1.0	2	92.9	99.9	131.2
6	C_6Pz-APTES/MCM-41	130	1.0	2	97.1	100	137.1

[a] Reaction conditions: 30 mmol PO and catalyst amount 10.3 wt.%.

[b] PC yield and selectivity were determined by GC.

[c] TOF: Moles of PC produced per mole of quaternary ammonium ion per hour

Table S2. Comparison of catalytic activity of DPzILs immobilized on modified MCM-41 with previously reported ILs-supported porous materials for CO_2 fixation.

Entry	Catalyst	Epoxide	Catalyst (wt.%)	T(°C)/t(h)/ CO_2(MPa)	Yield (%)	Ref.
1	MCM-41-S-ImBr	ECH	7.8	130/6/1.6	98.5	[4]
2	n-BImBr-MS41	AGE	11	110/6/2.1	97.5	[5]
3	mSiO_2-PIL-2	PO	20	120/6/2.0	86.0	[6]
4	MCM-41-IL	PO	8.0	130/6/3.0	96.1	[7]
5	MCM-41-Imi/All-Br	PO	1.6	150/8/1.5	68.8	[8]
6	MCM-41-Imi/COOH	PO	10	120/4/2.0	96.4	[9]

7	POM@ImTD-COF	SO	8.3	80/24/0.1	60	[10]
8	IPNs-CSU23/TBAB (TBAB as cocatalyst)	PO	-	25/48/0.1	99	[11]
9	SILEt^{+}Br^{-} (grafted on SBA-15)	SO	6.3	80/5/2.0	29.0	[12]
10	SILEt^{+}Br^{-} (grafted on SBA-15)	SO	6.3	90/5/2.0	50.0	[12]
11	POM@ImTD-COF (n-Bu_4NBr as cocatalyst)	SO	8.3	80/24/0.1	98.0	[10]
12	MCM-41-Imi/Br	SO	5.6	100/4/3.0	97.7	[13]
13	MCM-41-Imi/Br	SO	8.3	140/6/3.0	81.5	[13]
14	C_6Pz-APTES/MCM-41	PO	10.3	70/6/0.5	98.2	This work
15	C_6Pz-APTES/MCM-41	PO	5.4	90/3/1.0	97.9	This work

Table S3. NPA charge distribution and bond distance between bromide and cation

Sample	NPA charge of Br-	Br-N bond length (Å)
C_6Pz	-0.90339	4.392/3.904
C_3Pz	-0.90042	3.909/3.355

References

1. J. D. Ndayambaje, I. Shabbir, Q. Zhao, L. Dong, Q. Su and W. Cheng, *Catalysis Science & Technology*, 2024, **14**, 293-305.
2. M. Frisch, G. Trucks, H. Schlegel, G. Scuseria, M. Robb, J. Cheeseman, G. Scalmani, V. Barone, B. Mennucci and G. Petersson, *Phys. Rev. B: Condens. Matter Mater. Phys*, 1988, **37**, 785.

3. H. Du, Y. Ye, P. Xu and J. Sun, *Journal of CO_2 Utilization*, 2023, **67**, 102325.
4. Y. Wang, R. He, C. Wang and G. Li, *Reaction Kinetics, Mechanisms and Catalysis*, 2021, **134**, 823-835.
5. S. Udayakumar, M.-K. Lee, H.-L. Shim, S.-W. Park and D.-W. Park, *Catalysis Communications*, 2009, **10**, 659-664.
6. C. Yang, Y. Chen, X. Wang and J. Sun, *Journal of Colloid and Interface Science*, 2022, **618**, 44-55.
7. C. Cai, H. Wang and J. Han, *Applied Surface Science*, 2011, **257**, 9802-9808.
8. L. Muniandy, F. Adam, N. R. A. Rahman and E.-P. Ng, *Inorganic Chemistry Communications*, 2019, **104**, 1-7.
9. F. Gao, C. Ji, S. Wang, J. Dong, C. Guo, Y. Gao and G. Chen, *Colloids and Surfaces A: Physicochemical and Engineering Aspects*, 2023, **666**, 131304.
10. Y. Zhang, D.-H. Yang, S. Qiao and B.-H. Han, *Langmuir*, 2021, **37**, 10330-10339.
11. C. Ai, X. Ke, J. Tang, X. Tang, R. Abu-Reziq, J. Chang, J. Yuan, G. Yu and C. Pan, *Polymer Chemistry*, 2022, **13**, 121-129.
12. Z. Dokhaee, M. Ghiaci, H. Farrokhpour, G. Buntkowsky and H. Breitzke, *Industrial & Engineering Chemistry Research*, 2020, **59**, 12632-12644.
13. J. N. Appaturi and F. Adam, *Applied Catalysis B: Environmental*, 2013, **136-137**, 150-159.